Title

Stopping to reflect: Asymptotic static moving mirrors as quantum analogs of classical radiation

Authors

Good, Michael RR

Linder, Eric V

Publication Date

2023-10-01

DOI

10.1016/j.physletb.2023.138124

Physics Letters B 845 (2023) 138124

Contents lists available at ScienceDirect

Physics Letters B

journal homepage: www.elsevier.com/locate/physletb

Stopping to reflect: Asymptotic static moving mirrors as quantum analogs of classical radiation

Michael R.R. Good [a,b,c,*], Eric V. Linder [c,d]

[a] Physics Department, Nazarbayev University, Astana, Kazakhstan
[b] Leung Center for Cosmology and Particle Astrophysics, National Taiwan University, Taipei, Taiwan
[c] Energetic Cosmos Lab, Nazarbayev University, Astana, Kazakhstan
[d] Berkeley Center for Cosmological Physics & Berkeley Lab, University of California, Berkeley, CA, USA

ARTICLE INFO

Article history:
Received 11 June 2023
Received in revised form 27 July 2023
Accepted 10 August 2023
Available online 17 August 2023
Editor: B. Grinstein

Keywords:
Moving mirrors
Black hole evaporation
Acceleration radiation
Larmor power
Point charge

ABSTRACT

Radiation from an accelerating charge is a basic process that can serve as an intersection between classical and quantum physics. We present two exactly soluble electron trajectories that permit analysis of the radiation emitted, exploring its time evolution and spectrum by analogy with the moving mirror model of the dynamic Casimir effect. These classical solutions are finite energy, rectilinear (nonperiodic), asymptotically zero velocity worldlines with corresponding quantum analog beta Bogolyubov coefficients. One of them has an interesting connection to uniform acceleration and Leonardo da Vinci's water pitcher experiment.

1. Introduction

The mechanism of particle creation proposed by Hawking [1], whereby the gravitational field of a collapsing star in curved spacetime amplifies vacuum fluctuations into particle emission, bears striking resemblance to the radiation of particles from a perfect mirror in flat spacetime accelerated through the vacuum [2–4]. Particles of a massless quantum scalar field in $1+1$ dimensions [5,6] are created due to the acceleration of the mirror, which is an ideal point and boundary condition on the field [7–13], essentially a dynamical Casimir effect [14]. In this study, we demonstrate a functional duality and analog to an accelerated point charge in ordinary 3+1 space-time and its non-thermal radiation spectrum, revealing the particle creation correspondence.

Accelerating point charge radiation has been a subject of interest in physics for over a century [15], and it is of particular interest as a simple example of nonthermal radiation. Nonthermal radiation is ubiquitous in astrophysical phenomena, for example, and the particle number and angular spectral distribution may not be apparent. Furthermore, even evaporating black holes might emit non-thermal radiation, e.g. the recent [16]. Therefore a concrete relation between accelerated particle nonthermal radiation and the moving mirror "slicing" of the vacuum [17–20], especially in light of the well-established correspondence between moving mirrors and black hole horizons, is of interest.

The discovery of a clear association (generalized to non-thermal emissions) between the radiation from an electron and from a moving mirror became apparent via radiation reaction derived by Ford and Vilenkin in 1982 [8]. In 1995, Nikishov and Ritus [21] established a formal link through particle count, which further strengthened this connection. Ritus [22–25] later provided additional development on the Bogolyubov-current association. The relationship was next confirmed via Larmor power in Zhakenuly et al. [26]. One of the present authors has exploited the electron-mirror connection using explicit solutions; for instance, the connection between radiation power loss and kinetic power loss for an electron approaching the speed of light was demonstrated in [27], and in [28] an electron was treated as a mirror for a trajectory that asymptotically approaches a constant velocity. This article focuses on the interesting results for the electron-mirror relation for trajectories that come to a complete stop, giving finite energy, finite particle creation, and unitary evolution.

In Sec. 2, we review some elements of acceleration radiation for relativistic moving point charges, including Larmor power, Feynman power, and their connection to total energy emitted. We present the spectra for two different motions of point charges and the quantum analogs that have desirable properties and analytic

* Corresponding author.
E-mail addresses: michael.good@nu.edu.kz (M.R.R. Good), evlinder@lbl.gov (E.V. Linder).

https://doi.org/10.1016/j.physletb.2023.138124
0370-2693/

Bogolyubov coefficients in Sec. 3 and Sec. 4. In Sec. 5 we show the general correspondence between the classical bremsstrahlung and dynamical Casimir effect in energy, particle count, and spectral distribution. We summarize and discuss further areas for study in Sec. 6.

2. Acceleration radiation elements

In this section, we set up the various elements needed to compute the radiated power, energy, and spectral distribution of both an accelerating charge and from a moving mirror dynamical Casimir effect. We employ e and $\hbar$ for their classical and quantum contexts, respectively. We use units, $c = \mu_0 = \epsilon_0 = 1$, thus $e^2 = 4\pi\alpha_{\rm fs}\hbar$ where $\alpha_{\rm fs}$ is the fine structure constant.

2.1. Power and force

In classical electrodynamics [29], the power radiated and the radiation reaction force,

$$P = \frac{e^2\alpha^2}{6\pi}\,, \qquad F = \frac{e^2\alpha'(\tau)}{6\pi}\,, \tag{1}$$

are given by the relativistically covariant Larmor formula and the (magnitude of the) Lorentz-Abraham-Dirac (LAD) force. Here α is the proper acceleration, and the prime is a derivative with respect to the argument, in this case proper time τ.

2.2. Energy integrals

When the charged particle accelerates, energy is radiated, with the total energy found by integrating over coordinate time. That is, for particle velocity $v(t)$ the integrals

$$E = \int_{-\infty}^{\infty} P\,\mathrm{d}t = -\int_{-\infty}^{\infty} F\cdot v\,\mathrm{d}t, \tag{2}$$

demonstrate that the Larmor power, $P = e^2\alpha^2/6\pi$, and what we call the 'Feynman power' [30], $F\cdot v$, associated with the self-force (radiation reaction force), directly tell an observer the total energy emitted by a point charge along its time-like worldline. The total energy is finite as long as the proper acceleration is asymptotically zero; that is, the worldline must possess asymptotic inertia. We restrict ourselves to this case.

The negative sign demonstrates that the total work against the LAD force represents the total energy loss. That is, the total energy loss from radiation resistance due to Feynman power must equal the total energy radiated by Larmor power. We will demonstrate that the Larmor and Feynman powers themselves – the integrands – are not the same. Separately, it is a subtle matter that these powers are not applicable for asymptotically *non-inertial* rectilinear trajectories (which we do not consider here); see e.g. [27,31].

A third expression for the total energy can be employed to establish a link to quantum physics and verify consistency. This spectral consistency integrates over spectral modes,

$$E = \int_0^{\infty}\int_0^{\infty} \hbar p\,|\beta_{pq}|^2\,\mathrm{d}p\,\mathrm{d}q\,, \tag{3}$$

using the quantum analog moving mirror model, generalized to 3+1 dimensions using both sides of the 1+1 dimensional moving mirror, see e.g. [21,26].

The quantity β_{pq} is the beta Bogolyubov coefficient related to the creation/annihilation operators and p and q are the out-going and in-going frequencies, respectively, that describe the modes used to expand the field subject to the accelerating boundary.

2.3. Spectral distribution

The spectral distribution [32] of the total radiation energy E with respect to frequency ω and solid angle Ω is

$$\frac{\mathrm{d}I(\omega)}{\mathrm{d}\Omega} := \frac{\mathrm{d}^2 E}{\mathrm{d}\omega\,\mathrm{d}\Omega}\,, \tag{4}$$

see also [29]. For the radiation of a moving point charge (in our natural units – see e.g. Eq. 23.89 on page 911 of Zangwill [33] in SI units or Eq. 14.67 on page 701 of Jackson [29] in Gaussian units) this is given by the motion as

$$\frac{\mathrm{d}I(\omega)}{\mathrm{d}\Omega} = \frac{e^2\omega^2}{16\pi^3}\left|\hat{\boldsymbol{n}}\times\int_{-\infty}^{\infty} dt\,\dot{\boldsymbol{r}}(t)e^{i\phi}\right|^2. \tag{5}$$

Here ω is the frequency, $\boldsymbol{k} = \omega\hat{\boldsymbol{n}}$ the wave vector, $\mathrm{d}\Omega$ the solid angle, $\boldsymbol{r}$ the charge trajectory with velocity vector $\dot{\boldsymbol{r}}$, and $\phi = \omega t - \boldsymbol{k}\cdot\boldsymbol{r}(t)$. Defining $\hat{\boldsymbol{n}}\cdot\hat{\boldsymbol{r}} = \cos\theta$ and assuming straight line motion, we have

$$\frac{\mathrm{d}I(\omega)}{\mathrm{d}\Omega} = \frac{e^2\omega^2}{16\pi^3}\sin^2\theta\left|\int_{-\infty}^{\infty} dt\,\dot{r}(t)e^{i\phi}\right|^2. \tag{6}$$

Integrating this over solid angle $d\Omega = \sin\theta d\theta d\varphi$ and frequency ω will yield the total energy emitted.

We can also interpret the trajectory as not that of a point charge but an accelerating mirror (boundary) and compare the horizon radiation from this dynamical Casimir effect. Thus we can test that the classical energy emitted agrees with the quantum result from the Bogolyubov creation/annihilation coefficients, and also, contrast the Larmor and Feynman powers. This further provides a way to derive the spectrum angular distribution for particle production from a moving mirror trajectory.

2.4. Asymptotic rest

To pursue an understanding of the spectrum angular dependence for the quantum analog, we consider moving mirror trajectories that deliver finite total energy and particle count (ensuring all integrals are convergent). Asymptotically inertial mirrors have finite total energy, while mirrors that also are asymptotically static (eventually coming to rest with zero velocity) have finite particle count, entropy, and have unitary evolution (seen geometrically since all light rays reflect off the mirror and none are lost). Therefore we consider only cases with asymptotic rest.

The following list summarizes the only known trajectories possessing asymptotic rest with solved Bogolyubov coefficients.

- Walker-Davies [34]: but noninvertible $t(x)$.
- Arctx [35]: but nonfunctional particle count.
- **Self-Dual** [36]: time symmetric.
- **betaK** [37]: time antisymmetric.
- Schwarzschild-Planck [38,39] (also see [40]): fully evaporating black hole with unitarity.

None of these have previously had published solutions for the beta Bogolyubov coefficients using both mirror sides to obtain the 3+1 D analog (and hence classical particle motion). In the next two sections we present solutions for the two boldface trajectories – in particular as examples of time-symmetric vs antisymmetric motion, and the associated spectral distributions.

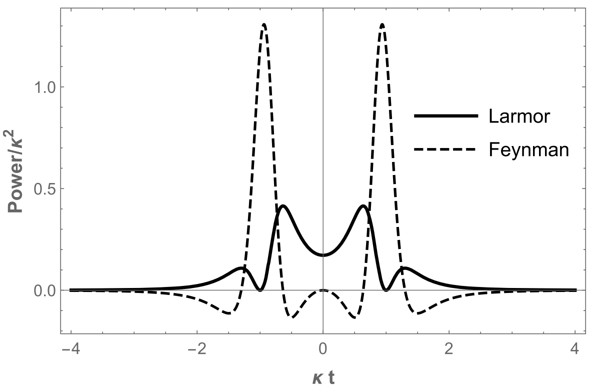

Fig. 1. The Larmor and Feynman powers for the self-dual trajectory (mirrors with $\hbar = 1$ or electrons with $e = 1$) are plotted vs time, with $v = 0.9$. A higher maximum velocity squeezes and heightens the peaks for both powers. The Feynman power plotted is $P_F = -F \cdot v$ so that the total area under the curve is positive, $E = \int P_F\, \mathrm{d}t$, see Eq. (2). Note the integrals under the curves are equal, giving the total energy radiated, Eq. (9).

3. Self-dual trajectory

The self-dual mirror trajectory [36]

$$x(t) = \frac{-v}{\kappa} \ln(\kappa^2 t^2 + 1) \,, \tag{7}$$

is even in time, and the self-dual nature means that the particle emission spectrum is equal on both sides of the mirror. The quantity v is the maximum speed of the mirror, occurring at $\kappa t = 1$. The quantity κ sets the scale of the acceleration (and the surface gravity of the black hole analog in the accelerating boundary correspondence).

The analog quantum Larmor power radiated is

$$P_L = \frac{2\hbar \kappa^2 v^2 \left(\kappa^4 t^4 - 1\right)^2}{3\pi \left[\left(\kappa^2 t^2 + 1\right)^2 - 4\kappa^2 t^2 v^2\right]^3} \,. \tag{8}$$

As expected, no power is radiated by a stationary mirror, $v = 0$, and none at the moment of maximum velocity when the acceleration is zero (i.e. when $\kappa t = 1$, as well as at asymptotically early and late times).

The Feynman force can be similarly calculated analytically but the expression is long. Fig. 1 plots the Larmor and Feynman powers vs time. The Larmor power is of course always positive, while the Feynman power from the radiation reaction force can be both positive and negative. The Feynman power crosses zero at maxima of the Larmor power. Both types of power asymptotically vanish rapidly.

Integrating over all time, Eq. (2), the total energy emitted is

$$E = \frac{\hbar \kappa}{24} \gamma v^2 \left(\gamma^2 + 3\right) \,, \tag{9}$$

where $\gamma = (1 - v^2)^{-1/2}$ is the Lorentz factor. Fig. 2 plots the total energy as a function of the maximum velocity. As the velocity approaches the speed of light, the Lorentz factor greatly increases the energy emitted.

For the Bogolyubov spectrum as found from the double-sided moving mirror, the result (see e.g. [35] for the details of the steps) is

$$|\beta_{pq}|^2 = \frac{16 v p q}{\pi^2 \kappa^2 \sigma \omega} \sinh\left(\frac{\pi v \sigma}{\kappa}\right) \left| K_{iv\frac{\sigma}{\kappa} + \frac{1}{2}} \left(\frac{\omega}{\kappa}\right)\right|^2 \,, \tag{10}$$

where $\sigma = p - q$ and $\omega = p + q$. The particle spectrum $N_p = \int dq\, |\beta_{pq}|^2$ is non-thermal, and has finite particle production, as seen in Fig. 3.

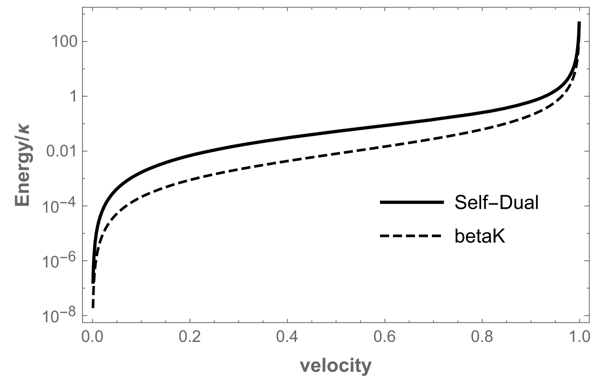

Fig. 2. The total energy scaling as a function of maximum velocity parameter is plotted for the self-dual trajectory (Eq. 9) and the betaK trajectory (Eq. 21) as mirrors with $\hbar = 1$.

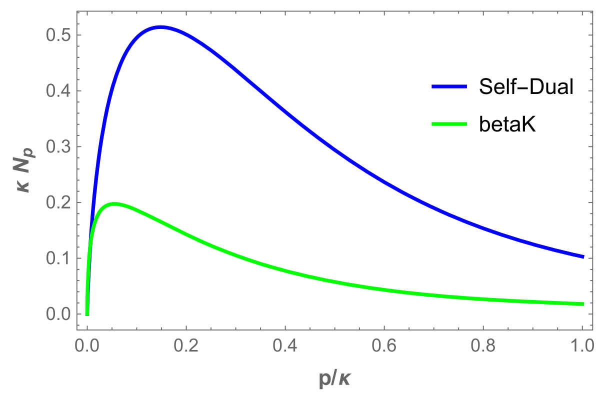

Fig. 3. A plot of particle spectrum $N(p)$ from the mirrors. This is the particle count as a function of the outgoing mirror mode frequency, p. Here the maximum velocity of each mirror is $v = v_0 = 0.9$.

For the spectral (angular) distribution, we use the self dual trajectory in Eq. (6), giving

$$\frac{\mathrm{d}I}{\mathrm{d}\Omega} = \frac{e^2 v \omega^2}{\kappa^2 \pi^3} \frac{1 - T^2}{2T} \sinh\left(\frac{\pi v T \omega}{\kappa}\right) \left| K_{\frac{1}{2} + \frac{i v T \omega}{\kappa}} \left(\frac{\omega}{\kappa}\right)\right|^2 \,, \tag{11}$$

where $T \equiv \cos\theta$. Some details of the derivation are given in Appendix A. Note the similarity to the form of the beta Bogolyubov coefficients, but with added angular dependence (see the next subsection for further discussion).

Figs. 4 and 5 plot the spectral distribution in a 3D view. Notice there is no radiation in the forward or backward $T \to \pm 1$ ($\theta \to [0, \pi]$) directions. This is expected of straight-line bremsstrahlung [41]. The spectral distribution in the $T \to 0$ ($\theta \to \pi/2$) limit is:

$$\lim_{T \to 0} \frac{\mathrm{d}I}{\mathrm{d}\Omega} = \frac{e^2 v^2 \omega^2}{4\pi \kappa^2} e^{-2\omega/\kappa} \,, \tag{12}$$

which demonstrates a radiation allotment in directions perpendicular to the motion that is exponentially suppressed at high frequencies. The spectrum, $I(\omega)$, can be numerically found by integrating the spectral distribution, Eq. (11), over solid angle. See Fig. 6 for an illustration.

The spectral distribution can be directly integrated over solid angle and frequency to obtain the total energy

$$E = \int_0^\infty \mathrm{d}\omega \int_{-1}^{1} \mathrm{d}T \int_0^{2\pi} \mathrm{d}\varphi\, \frac{\mathrm{d}I}{\mathrm{d}\Omega} \tag{13}$$

$$= \frac{e^2 \kappa}{24} \gamma v^2 \left(\gamma^2 + 3\right) \,. \tag{14}$$

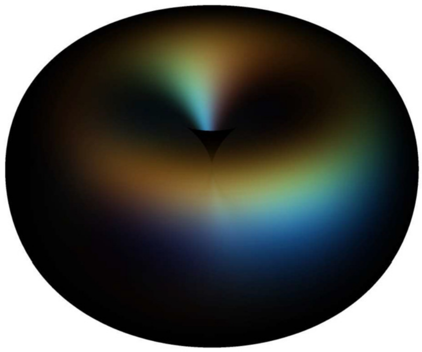

Fig. 4. 3D view of the radiated spectrum angular distribution $\mathrm{d}I/\mathrm{d}\Omega$ from electron motion corresponding to the self dual trajectory. Here we use unit charge, natural units, and $\omega = \kappa = 1$. The maximum speed of the charge is $v = 0.95$. Note the expected property of zero radiation directly in the forward direction.

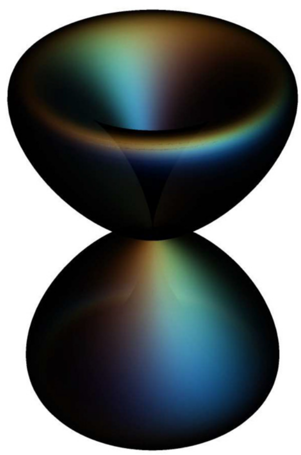

Fig. 5. As Fig. 4 but for $\omega = 4$, $\kappa = 1$, showing the high-frequency exponential suppression.

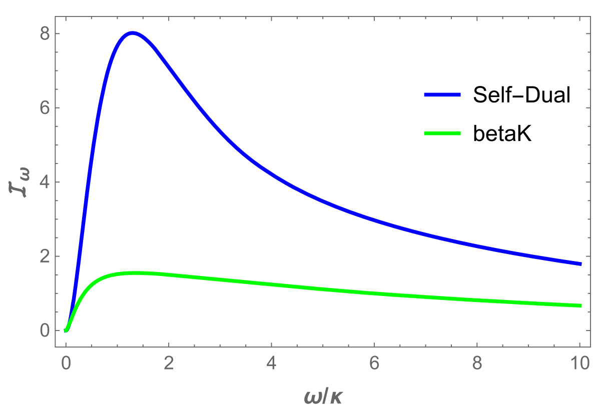

Fig. 6. For the electrons, a plot of energy spectrum $I(\omega)$, which numerically integrates the spectral distributions for the self-dual, Eq. (11), and betaK, Eq. (22), cases over solid angle Ω with $e = 1$. The vertical axis has been multiplied by 10^3 for readability. Here the maximum velocity of each case is $v = v_0 = 0.9$.

This agrees with Eq. (9) up to $4\pi\alpha_{\rm fs}$, as expected.

4. betaK trajectory

The betaK trajectory [37]

$$x(t) = \frac{-v_0}{\kappa} \sinh^{-1} \kappa t\,, \tag{15}$$

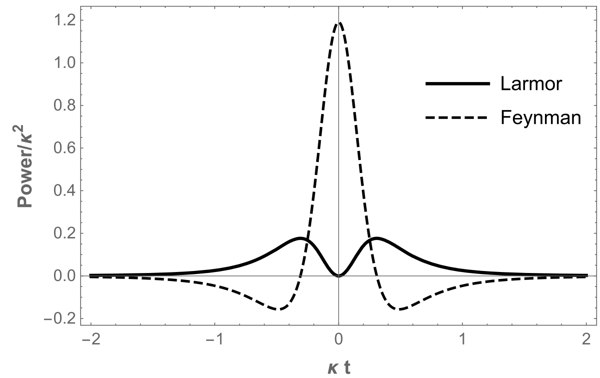

Fig. 7. The Larmor and Feynman powers for the betaK electron trajectory are plotted vs time, with $v_0 = 0.9$. Like the self-dual trajectory, a higher v_0 narrows and heightens the peaks for both powers. For illustration, the Feynman power plotted is $P_F = -F \cdot v$ so the total area under the curve is positive; $e = 1$. The areas under the curves are equal, giving the total energy radiated, Eq. (19).

by contrast is odd in time, and gives more tractable solutions than the Walker-Davies or Arctx models. Furthermore it has an interesting relation to uniform acceleration in 3+1 D (though not in the 1+1 D mirror case).[1] Its name arises because this trajectory has exactly solvable beta Bogolyubov coefficients involving a modified Bessel function K in the moving mirror model, giving finite energy and finite particle production.

This trajectory equation arises as well for a particle shot horizontally from the origin with an initial velocity v_0 (which is also the maximum velocity) encountering a constant vertical acceleration. Indeed, this is similar to the recently rediscovered "Leonardo da Vinci's water pitcher" that moves horizontally at constant speed v spilling water in a uniform gravitational field [42] – but here we consider relativistic speeds. The derivation appears in Appendix B.

Note that in the relativistic case, despite no horizontal force the particles (water drops) do not have constant horizontal velocity: due to the coupling of horizontal and vertical motions through the Lorentz factor a horizontal acceleration is induced as made clear in Appendix B.

The Larmor power radiated by a charge with the betaK trajectory is

$$P_L = \frac{e^2\alpha^2}{6\pi} = \frac{e^2\kappa^2}{6\pi}\gamma^6\left(v_0^2 - V^2\right)\frac{V^4}{v_0^4}\,, \tag{16}$$

where the velocity is

$$V(t) \equiv \dot{x}(t) = \frac{-v_0}{\sqrt{\kappa^2 t^2 + 1}}\,. \tag{17}$$

The speed $|V| \le |v_0|$ so the power always remains nonnegative. For this time antisymmetric trajectory, the power has only one maximum on each side of $t = 0$ and no zeros for finite $t \neq 0$. The Feynman power is

$$P_F = \frac{e^2\alpha^2}{6\pi}\left[2 - \frac{V^2(1 - v_0^2)}{v_0^2 - V^2}\right]. \tag{18}$$

The total energy, using Eq. (2), is

$$E = \frac{e^2\kappa}{48}\gamma_0^3 v_0^2\,. \tag{19}$$

See Fig. 2 for the energy and Fig. 7 for the Larmor and Feynman powers.

[1] We thank Ahmad Shariati for pointing this out.

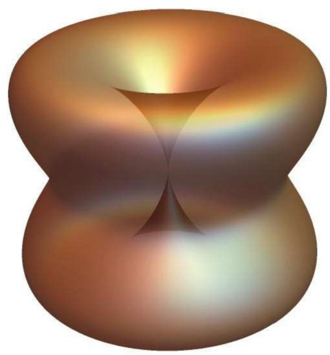

Fig. 8. 3D view of the radiated spectrum angular distribution $\mathrm{d}I/\mathrm{d}\Omega$ from the electron motion corresponding to the betaK trajectory. Here we use unit charge, natural units, and $\omega=\kappa=1$. The maximum speed of the charge is $v_0=0.95$.

The Bogolyubov spectrum as found from the double-sided moving mirror is

$$|\beta_{pq}|^2 = \frac{8v_0^2 pq}{\pi^2\kappa^2\omega^2}\cosh\left(\pi v_0 \frac{\sigma}{\kappa}\right)\left|K_{iv_0\frac{\sigma}{\kappa}}\left(\frac{\omega}{\kappa}\right)\right|^2 , \tag{20}$$

where $\sigma=p-q$ and $\omega=p+q$. This spectrum is not thermal. Note the similarities, but also subtle differences with the self-dual case, Eq. (10). The energy is confirmed by associating a quantum $\hbar p$ (where p is the outgoing frequency mode) and integrating using Eq. (3), which yields the analog of Eq. (19),

$$E = \frac{\hbar\kappa}{48}\gamma_0^3 v_0^2. \tag{21}$$

The particle spectrum $N_p=\int dq\,|\beta_{pq}|^2$ is shown in Fig. 3.

Using the betaK trajectory within classical electrodynamics [29], we find the spectral distribution,

$$\frac{\mathrm{d}I}{\mathrm{d}\Omega} = \frac{e^2v_0^2\omega^2}{4\kappa^2\pi^3}(1-T^2)\cosh\left(\pi v_0 T\frac{\omega}{\kappa}\right)\left|K_{iv_0T\frac{\omega}{\kappa}}\left(\frac{\omega}{\kappa}\right)\right|^2 , \tag{22}$$

where $T=\cos\theta$. Again a relation between the classical spectral distribution and quantum beta Bogolyubov coefficient is apparent; we address this in Section 5.

The energy spectrum $I(\omega)$ is shown in Fig. 6. Integration of Eq. (22) over $\mathrm{d}\omega\,\mathrm{d}\Omega$ agrees with the total energy of Eq. (19). Like the self-dual case, as expected, there is no radiation in the forward or backward $T\to\pm1$ ($\theta\to[0,\pi]$) directions. See Fig. 8 for a 3D view of the spectral distribution. The spectral distribution in the $T\to 0$ ($\theta\to\pi/2$) limit is:

$$\lim_{T\to 0}\frac{\mathrm{d}I}{\mathrm{d}\Omega} = \frac{e^2v_0^2\omega^2}{4\pi^3\kappa^2}\left[K_0\left(\frac{\omega}{\kappa}\right)\right]^2 \tag{23}$$

$$\approx \frac{e^2v_0^2\omega}{8\pi^2\kappa}\, e^{-\frac{2\omega}{\kappa}} , \tag{24}$$

again showing the high-frequency exponential suppression, wherein the second line we have expanded around large ω/κ.

The betaK trajectory is well-motivated, physically intuitive, and potentially realizable in the laboratory as it is straightforwardly the horizontal component of an electron's motion subject to an initial horizontal velocity and constant vertical force. In the following section, we use betaK's analytic tractability to help confirm the duality between the classical point charge and the quantum moving mirror.

5. Classical-quantum correspondence

We have seen that at the level of total energy, there is an agreement (up to the pre-factor $4\pi\alpha_{\rm fs}$) between the charge radiation approach and the moving mirror Bogolyubov coefficient approach,

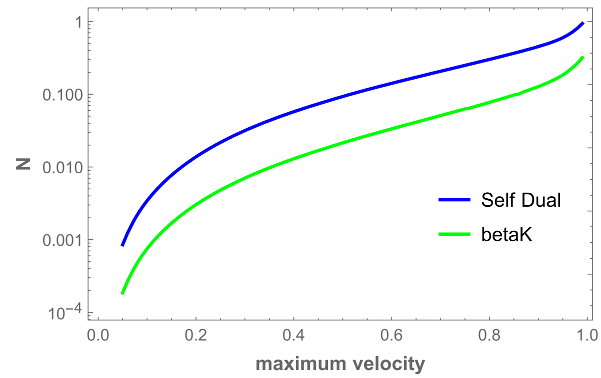

Fig. 9. A plot of total finite particle count of the radiation particles created by the two mirrors, using Eq. (26), for maximum velocity ranging from 0.05 to 0.99.

$$E = \int_0^\infty \mathrm{d}\omega \int_{-1}^{1}\mathrm{d}T\int_0^{2\pi}\mathrm{d}\varphi\,\frac{\mathrm{d}I}{\mathrm{d}\Omega} \Leftrightarrow \int_0^\infty\int_0^\infty \hbar p\,|\beta_{pq}|^2\,\mathrm{d}p\,\mathrm{d}q\,. \tag{25}$$

We can further see that the agreement extends to the particle count,

$$N = \int \frac{1}{\hbar\omega}\frac{\mathrm{d}I}{\mathrm{d}\Omega}\,\mathrm{d}\Omega\,\mathrm{d}\omega \Leftrightarrow \frac{1}{2}\int\int |\beta_{pq}|^2\,\mathrm{d}p\,\mathrm{d}q\,. \tag{26}$$

The factor $1/\omega$ converts particle energy to particle number, and the factor $1/2$ arises because while both sides of the mirror are employed in the correspondence, an observer could only see one side. See Fig. 9 for an illustration of particle count.

As mentioned in Section 3 and Section 4 the connection persists at the level directly between the spectral distribution and the beta Bogolyubov coefficient, i.e. the integrands. The steps to obtain the exact relation are as follows. First, the Jacobian going from $\{p,q\}$ coordinates to $\{\omega,T\}$ coordinates is $\omega/2$. Recall that $\mathrm{d}\Omega=\sin\theta\,\mathrm{d}\theta\,\mathrm{d}\varphi$ and that $\mathrm{d}T\equiv\mathrm{d}(\cos\theta)=\sin\theta\,\mathrm{d}\theta$ and the $\mathrm{d}\varphi$ integral simply contributes 2π. Finally, the parity is reversed on opposite sides of the mirror so that one side is related to the other by $T\leftrightarrow -T$, so we write

$$\int_{-1}^{+1} dT\,\frac{dI}{d\Omega} = \frac{1}{2}\left[\int_{-1}^{+1} dT\,\frac{dI(T)}{d\Omega} + \int_{-1}^{+1} dT\,\frac{dI(-T)}{d\Omega}\right]. \tag{27}$$

Putting all the elements together delivers the correspondence

$$|\beta_{pq}|^2 \;\leftarrow\; \frac{4\pi}{e^2\omega^2}\left[\frac{\mathrm{d}I}{\mathrm{d}\Omega}(\omega,\cos\theta)+\frac{\mathrm{d}I}{\mathrm{d}\Omega}(\omega,-\cos\theta)\right]. \tag{28}$$

This can be verified directly for the solutions given for the two trajectories. Note that the correspondence formally goes in only one direction, from charge radiation to moving mirror, as the beta Bogolyubov coefficient has no angular information on the in-going and out-going modes. Only once we introduce an angle θ such that $p=\omega(1+\cos\theta)/2$ and $q=\omega(1-\cos\theta)/2$, hence $p+q=\omega$ and $\sigma\equiv p-q=\omega\cos\theta$, can we go the other way.

Such a classical-quantum correspondence is very useful, but we emphasize that it does not capture all quantum effects. While the particle production can be computed classically, this neglects quantum effects when the radiation (photon) energy becomes comparable to the particle (electron) energy, e.g. the radiation wavelength is smaller than the charge de Broglie wavelength.

6. Conclusions

We have solved for the accelerating point charge radiation – its energy, particle count, and spectral angular distribution – of two trajectories that asymptotically come to complete stop, compatible with finite total particle emission. As Feynman [30] has emphasized,

Larmor's power is only valid for cyclic motions, or at least motions which do not grow forever in time.

The betaK and Self-Dual trajectories fulfill that condition, and these two solutions inspired by the accelerating boundary (moving mirror) analog are the only known rectilinear solutions with exactly soluble spectra, finite energy, and finite particle count. This allows comparison of classical and quantum systems directly.

The main results presented include:

- We have found the time dependence of radiative solutions. One utility of an exact solution for moving point charge radiation is that in QED, time-dependent computations are notoriously difficult. Here the dynamics are explicit in the applicable Larmor and Feynman powers.
- We have demonstrated consistency between the total energy derived in terms of the Larmor power, the Feynman power, and the quantum Bogolyubov coefficients.
- We have derived the spectral distributions of these two accelerating, but asymptotically static, motions analytically, and further shown consistency with the total energy emission and total particle count. In addition to 3D plots of the radiation angular distribution we discussed the angular limits (e.g. the forward and transverse emission) and high frequency limits.
- We have laid out explicitly a quantum-classical correspondence to the moving mirror model, mapping between the classical spectral distribution and the quantum Bogolyubov coefficients.

The demonstrated consistency and explicit correspondence enhances the utility of the moving mirror model by showing its role as a point charge analog. Thus the accelerated boundary correspondence of the moving mirror to black hole radiation may potentially point to a connection to accelerating charge radiation via a Hawking-Feynman-Larmor correspondence.

This is an exciting prospect for future directions. It may be tractable to link directly these electron trajectories to curved spacetime counterparts, revealing spacetime metrics that radiate with similar nonthermal spectra (or reveal charge motions that could show a period of thermal emission). Further, given that a connection for beta decay to a moving mirror analog has been made [43–45], other well-known QED scattering processes might correspond at lowest order to one of the solutions given. Asymptotic rest, with its finite particles and unitarity, could be a powerful tool, and it would be interesting to develop further solutions, such as the Schwarzschild-Planck radiation [38–40] to compare accelerating electron and black hole radiation in the thermal limit.

Declaration of competing interest

The authors declare that they have no known competing financial interests or personal relationships that could have appeared to influence the work reported in this paper.

Data availability

No data was used for the research described in the article.

Acknowledgements

Funding comes in part from the FY2021-SGP-1-STMM Faculty Development Competitive Research Grant No. 021220FD3951 at Nazarbayev University. This work is supported in part by the Energetic Cosmos Laboratory, and in part by the U.S. Department of Energy Office of Science, Office of High Energy Physics, under contract no. DE-AC02-05CH11231.

Appendix A. Spectral distribution calculation

To show how one can go from the formula for the spectral distribution, Eq. (6), to the modified Bessel function result we illustrate the steps for the self dual case. The integral has the form

$$A \equiv \int_{-\infty}^{+\infty} dt\, \dot{x}\, e^{i\omega(t - x\cos\theta)}\ . \tag{A.1}$$

Substituting in the self dual expressions for $x(t)$ from Eq. (7), and $\dot{x}$, and writing $T \equiv \cos\theta$ we have

$$A = \int_{-\infty}^{+\infty} dt\, \frac{-2v\kappa t}{\kappa^2 t^2 + 1}\, e^{i\omega[t + (vT/\kappa)\ln(\kappa^2 t^2 + 1)]} \tag{A.2}$$

$$= \frac{-2v}{\kappa} \int_{-\infty}^{+\infty} ds\, s(s^2+1)^{-1+i\omega vT/\kappa}\, e^{i\omega t} \tag{A.3}$$

$$= \frac{-4iv}{\kappa} \int_{0}^{\infty} ds\, s(s^2+1)^{-1+i\omega vT/\kappa}\, \sin\frac{\omega s}{\kappa}\ . \tag{A.4}$$

In the second line we have taken the exponential of the log term, and defined $s = \kappa t$, while in the third line we have used that we must take the odd part of the remaining exponential to give an even integrand over the symmetric range of integration.

This integral can be evaluated through Gradshteyn & Ryzhik 3.771.5 [46], resulting in

$$A = \frac{4v}{\kappa\sqrt{\pi}} \left(\frac{\omega}{2\kappa}\right)^{1/2 - i\omega vT/\kappa} \sinh(\pi\omega vT/\kappa)\, \Gamma\left(\frac{i\omega vT}{\kappa}\right) \times K_{1/2 + i\omega vT/\kappa}\left(\frac{\omega}{\kappa}\right)\ . \tag{A.5}$$

The modulus squared, using that $|\Gamma(ix)|^2 = \pi/(x\sinh x)$, is

$$|A|^2 = \frac{8v}{\kappa^2 T} \sinh(\pi\omega vT/\kappa) \left|K_{1/2 + i\omega vT/\kappa}\left(\frac{\omega}{\kappa}\right)\right|^2\ . \tag{A.6}$$

For the betaK case we proceed similarly, noting that since $\dot{x}$ is even in time in that case we must take the even part of the exponential (i.e. cosine).

Appendix B. Leonardo's pitcher: from electron to betaK

The motion of a relativistic particle with unit mass subject to an external force comes from the action[2]

$$S = -\int dt\, \left(\sqrt{1 - v^2} + Fx\right)\ . \tag{B.1}$$

For a force dependent only on position the equations of motion are simply

$$\alpha = \frac{d}{dt} \frac{v}{\sqrt{1 - v^2}} \equiv \frac{d(\gamma v)}{dt} \tag{B.2}$$

$$= (0, \alpha_y, 0)\ , \tag{B.3}$$

[2] This is a first prototypical system of a relativistic Lagrangian (see e.g. page 323 of [47]).

where the last line holds for purely vertical force, and we will take $\alpha_y = \text{const}$ (e.g. gravity in Leonardo's water pitcher experiment). Finally, we take the initial velocity to be purely horizontal, $v = (v_0, 0, 0)$.

The results are simple – nonuniform motion in the horizontal direction due to the relativistic boost factor γ, and hyperbolic motion under constant acceleration in the vertical direction – but worth quickly going through to reveal the form of nonuniformity.

The z direction is trivial: as there is no initial velocity, nor subsequent acceleration, in this direction then Eq. (B.2) guarantees that $z(t) = z(0)$ and we can ignore this dimension. In the x (horizontal) direction, Eq. (B.2) gives

$$\gamma(t) v_x(t) = \gamma_0 v_0 \,, \tag{B.4}$$

and the key point is that while nonrelativistically one would simply have $v_x(t) = v_0$, i.e. uniform motion, the Lorentz factor γ couples in the y motion (recall $\gamma = 1/\sqrt{1 - v_x^2 - v_y^2}$), which is accelerated. This results in nonuniform motion horizontally.

We can relate v_x and v_y, and solve for both motions by squaring Eq. (B.4) to get

$$v_x^2 = (1 - v_y^2) v_0^2 \,. \tag{B.5}$$

This immediately tells us that v_x has its maximum value at the initial time, so $v_y(t) < v_0 = v_y(0)$. That is, the vertical acceleration effectively causes a horizontal deceleration!

In the y (vertical) direction, the equation of motion gives $\gamma v_y = \alpha_y t$ so

$$v_y = \frac{\kappa t}{\sqrt{1 + (\kappa t)^2}} \,. \tag{B.6}$$

At late times this approaches the speed of light. To presage the betaK mirror analogy we have written $\kappa \equiv \alpha_y/\gamma_0$. Finally, with Eq. (B.5) we obtain the horizontal velocity

$$v_x = \frac{v_0}{\sqrt{1 + (\kappa t)^2}} \,, \tag{B.7}$$

which indeed decelerates from its initial value to zero. Again presaging the mirror analog, we will end up with an asymptotically static mirror defined by the 1D horizontal motion.

Integrating the velocities gives the trajectories, with

$$y(t) = \kappa^{-1}\sqrt{1 + \kappa^2 t^2} - \kappa^{-1} \,, \tag{B.8}$$

revealing hyperbolic motion in the vertical direction. In the horizontal direction,

$$x(t) = \frac{v_0}{\kappa} \sinh^{-1} \kappa t \,, \tag{B.9}$$

exactly (after a trivial sign flip on initial velocity) the betaK trajectory, Eq. (15).

References

[1] S. Hawking, Commun. Math. Phys. 43 (1975) 199.
[2] B.S. DeWitt, Phys. Rep. 19 (1975) 295.
[3] S.A. Fulling, P.C.W. Davies, Proc. R. Soc. Lond. A 348 (1976) 393.
[4] P. Davies, S. Fulling, Proc. R. Soc. Lond. A 356 (1977) 237.
[5] N. Birrell, P. Davies, Quantum Fields in Curved Space, Cambridge Monographs on Mathematical Physics, Cambridge Univ. Press, Cambridge, UK, 1984.
[6] A. Fabbri, J. Navarro-Salas, Modeling Black Hole Evaporation, Imperial College Press, 2005.
[7] W.R. Walker, Phys. Rev. D 31 (1985) 767.
[8] L. Ford, A. Vilenkin, Phys. Rev. D 25 (1982) 2569.
[9] R.D. Carlitz, R.S. Willey, Phys. Rev. D 36 (1987) 2327.
[10] P. Chen, G. Mourou, Phys. Rev. Lett. 118 (2017) 045001, arXiv:1512.04064 [gr-qc].
[11] P. Chen, et al., AnaBHEL, arXiv:2205.12195 [gr-qc], 2022.
[12] M.R.R. Good, A. Lapponi, O. Luongo, S. Mancini, Phys. Rev. D 104 (2021) 105020, arXiv:2103.07374 [gr-qc].
[13] P. Chen, G. Mourou, Phys. Plasmas 27 (2020) 123106, arXiv:2004.10615 [physics.plasm-ph].
[14] G.T. Moore, J. Math. Phys. 11 (1970) 2679.
[15] J. Larmor, Lond. Edinb. Dublin Philos. Mag. J. Sci. 44 (1897) 503.
[16] A.A. Svidzinsky, Phys. Rev. D 107 (2023) 024038, arXiv:2301.13131 [gr-qc].
[17] K.-N. Lin, P. Chen, arXiv:2107.09033 [gr-qc], 2021.
[18] I.A. Reyes, Phys. Rev. Lett. 127 (2021) 051602, arXiv:2103.01230 [hep-th].
[19] K.-N. Lin, P. Chen, arXiv:2212.00550 [gr-qc], 2022.
[20] I. Akal, Y. Kusuki, N. Shiba, T. Takayanagi, Z. Wei, Phys. Rev. Lett. 126 (2021) 061604, arXiv:2011.12005 [hep-th].
[21] A. Nikishov, V. Ritus, J. Exp. Theor. Phys. 81 (1995) 615.
[22] V. Ritus, J. Exp. Theor. Phys. 87 (1998) 25, arXiv:hep-th/9903083.
[23] V. Ritus, Int. J. Mod. Phys. A 17 (2002) 1033.
[24] V. Ritus, J. Exp. Theor. Phys. 97 (2003) 10, arXiv:hep-th/0309181.
[25] V.I. Ritus, Usp. Fiz. Nauk 192 (2022) 507.
[26] A. Zhakenuly, M. Temirkhan, M.R.R. Good, P. Chen, Symmetry 13 (2021) 653, arXiv:2101.02511 [gr-qc].
[27] M.R.R. Good, C. Singha, V. Zarikas, Entropy 24 (2022) 1570, arXiv:2211.00264 [gr-qc].
[28] M.R.R. Good, Y.C. Ong, Physics 5 (2023) 131, arXiv:2302.00266 [gr-qc].
[29] J.D. Jackson, Classical Electrodynamics, 3rd ed., Wiley, New York, NY, 1999.
[30] R.P. Feynman, in: F.B. Morinigo, W.G. Wagner, B. Hatfield (Eds.), Feynman Lectures on Gravitation, 1996.
[31] A.K. Singal, Symmetry 12 (2020) 1833.
[32] J.S. Schwinger, Phys. Rev. 75 (1949) 1912.
[33] A. Zangwill, Modern Electrodynamics, Cambridge Univ. Press, Cambridge, 2013.
[34] W.R. Walker, P.C.W. Davies, J. Phys. A, Math. Gen. 15 (1982) L477.
[35] M.R.R. Good, P.R. Anderson, C.R. Evans, Phys. Rev. D 88 (2013) 025023, arXiv:1303.6756 [gr-qc].
[36] M.R.R. Good, E.V. Linder, Phys. Rev. D 96 (2017) 125010, arXiv:1707.03670 [gr-qc].
[37] M.R. Good, E.V. Linder, Phys. Rev. D 99 (2019) 025009, arXiv:1807.08632 [gr-qc].
[38] M.R. Good, E.V. Linder, F. Wilczek, Phys. Rev. D 101 (2020) 025012, arXiv:1909.01129 [gr-qc].
[39] M.R.R. Good, E.V. Linder, New J. Phys. 23 (2021) 043007, arXiv:2003.01333 [gr-qc].
[40] A. Moreno-Ruiz, D. Bermudez, Class. Quantum Gravity 39 (2022) 145001, arXiv:2112.00194 [gr-qc].
[41] D.J. Griffiths, Introduction to Electrodynamics, 4th ed., Pearson, Boston, MA, 2013, re-published by Cambridge University Press, in 2017.
[42] M. Gharib, C. Roh, F. Noca, Leonardo 21 (2022).
[43] M.R.R. Good, P.C.W. Davies, Found. Phys. 53 (3) (2023) 53, https://doi.org/10.1007/s10701-023-00694-x.
[44] M.H. Lynch, M.R.R. Good, arXiv:2211.14774 [nucl-ex], 2023.
[45] E. Ievlev, M.R.R. Good, Physics 5 (3) (2023) 797–813, https://doi.org/10.3390/physics5030050.
[46] I. Gradshteyn, I. Ryzhik, Table of Integrals, Series, and Products, 7th ed., Academic Press, San Diego, CA, 1994.
[47] H. Goldstein, Classical Mechanics, Addison-Wesley, 1980.